Chapter 5

Optical Waveguide for Measurement Application

Prashant Bansilal Patel and Satish T. Hamde

Additional information is available at the end of the chapter

http://dx.doi.org/10.5772/intechopen.76781

Abstract

The chapter provides the analysis of the behaviour of Mach Zehnder interferometer waveguide (MZIW) sensing structure and establishes the general design principles. Photonics interferometers have been widely used because of their highly sensitive detection technique. The present study is based on the MZIW structure for sensing application and deals with interferometer single-mode transmission. Theoretically, short wavelength and high difference in index ($\Delta\eta$) results in the low depth of the evanescence wave and increase in sensitivity. MZIW under consideration is very small in size hence it is very difficult to guide the light into waveguide. The output monitor detection sensitivity of the entire MZI structure depends on light-guiding efficiency. To maintain minimum losses at various micro-branches of the entire MZIW structure, effective light propagation is important and it is a critical parameter of the entire interferometer. Various tests have been carried out to study the effects of the Y branch angle variation on light guiding into the MZIW structure especially in measurement application.

Keywords: interferometer, light propagation, waveguide

1. Introduction

Guided wave optics has revolutionized the photonic sensing technology. It covers both fibre and integrated optics technology. Photonics technology improves optical communication and minimizes the optical components used for communication as well as measurement applications [1]. Silicon nano-photonics waveguides strongly confine light in a submicron waveguide structure which has following advantages.

(i) allows sharp bends due to which compact and tiny components can be analysed and characterized;

(ii) gives tremendous reduction in footprints, which in turns open up new areas for the large-scale integration of photonics component circuits.

The fabrication of photonics circuits can be done on the similar line of complementary metal-oxide-semiconductor (CMOS) circuits [2]. Due to the similarity, CMOS compatibility opens up options for the interface of photonics functions with electronics functions. Photonics sensing technology has now gained a place in the vast portfolio of practical measurement technologies [3, 4].

However, current innovations in the photonics technique to manipulate the light are continue to provide both opportunity and challenge to the micro-optical components used in rapid measurement and sensing technologies. The development in the modern photonics sensors is due to the advances made in the LASER and optical fibre technology. The progress in the microelectronics field accelerated the growth in silicon as well as polymer-based photonics devices.

Photonics technology also enhances precision as well as accuracy of the measurement. Photonics-based sensors reduce the measurement time which is not possible using conventional available techniques. The application of nanotechnology in the field of biology and biomedical field is known as bio-nano-technology or nano-bio-technology [5]. This technology gives rise to new devices and systems having improved sensitivity and accuracy for measurement application. Interferometer analysis using the Y branch is highlighted in this chapter for the MZIW structure and the general conclusions on optimization are drawn [6].

2. Interferometer technique

In interferometer phenomenon, two similar input waves are superimposed at an output waveguide to detect the phase difference between them. If the two waves are in phase, their electrical fields gets added (this is called as constructive interference). If they are out of phase (phase shift is 180° between them), the electric field received at the output waveguide gets cancelled (this is called as destructive interference).

Various interferometer configurations like Mach Zehnder interferometer, Fabry Perot interferometer and Michelson interferometer have been realized using optical methods. Out of all above techniques, the main consideration in this chapter is given to Mach Zehnder interferometer [7, 8].

3. Mach Zehnder interferometer waveguide (MZIW)

Interferometer is most suitable technique for analytical measurement with real-time interaction monitoring. Our main purpose is to provide the optimization and testing of MZIW. Interferometer based on MZIW consists of input waveguide structure (left Y branch) and output waveguide structure (right Y branch) [8]. In interferometer measurement, input light is equally guided into the two waveguides and light is recollected into the single

http://dx.doi.org/10.5772/intechopen.76781

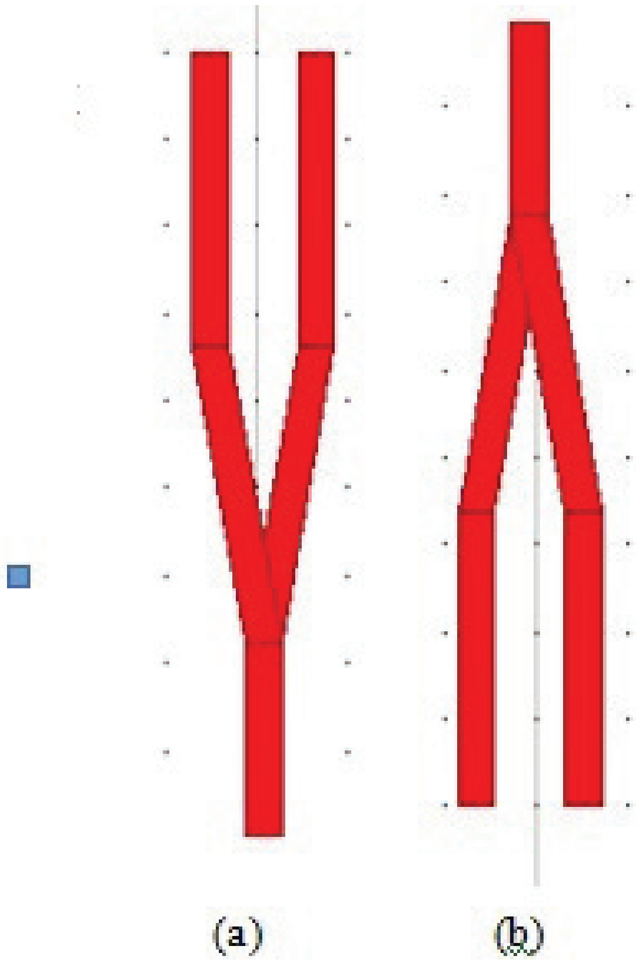

Figure 1. *Y* branches (a) Branch [1-2] (b) Branch [2-1].

waveguide as shown in **Figure 1**. One branch is 1-2 and other is the 2-1 branch. The sensing reaction changes the refractive index of sensing waveguide and it changes the speed (phase) of light [9]. The light intensity changes due to the optical interference at the output waveguide (2-1 branch) [10]. **Figure 1** demonstrates one-input and two-output (1-2 branches) and two-input one-output (2-1 branch)-type micro-*Y* branch for the MZIW structure. Many optical evanescent wave sensors in various forms have been used for highly sensitive sensing applications and MZIW is one class of such sensors. MZIW has been designed using one *Y* and one inverted *Y* branch to form an entire waveguide structure [11].

The simplest light waveguide component is the *Y* branch and is a three-port device that acts as a light divider, *Y* branch (1-2) and light collector and inverted *Y* branch (2-1) [12]. **Figure 1** shows a *Y* branch made by splitting a planer waveguide into two branches bifurcating at some angle. These components are very much similar to a fibre optic coupler which can also act as a power splitter except that it has only three ports. Conceptually it differs considerably from a fibre coupler since there is no coupling region in which modes of two different waveguides overlap. Function of the *Y* branch is very simple. With reference to **Figure 1**, in the branch region the waveguide is thicker and supports higher-order modes. However the geometrical symmetry forbids the excitation of asymmetric modes. If the thickness is changed gradually in an adiabatic manner, even higher-order symmetric modes are not excited, and power is divided into two branches without much loss. In practice, a sudden opening of the gap violates the adiabatic condition, resulting in insertion losses associated with any *Y* branch. These losses depend on the branching angle θ and increases as angle θ increases.

In practice, what attracts our attention is the presence of a number of relatively primitive, that is, straight and curved waveguides. As it was mentioned earlier, the layout is very coarse and the light interactions actually occur just on a small fraction of the layout. For this reason waveguides are also called as micro-waveguides and the branches are also called as micro-branches. Various types of MZIW structures have been designed for sensing applications.

We have used beam propagation method (BPM) for the analysis of MZIW [13]. The physical propagation requires important information about the distribution of refractive index η(x, y, z) and input wave field, η(x, y, z = 0). From this we can detect the wave field throughout the rest of the domain u (x, y, z > 0).

In addition to above data, the BPM algorithm requires additional information in the form of numerical parameters like:

(i) finite computation domain $\{X \in (x_{min}, x_{max})\}$, $\{Y \in (y_{min}, y_{max})\}$, $\{Z \in (z_{min}, z_{max})\}$,

(ii) transverse grid size Δx and Δy,

(iii) longitudinal step size Δz.

Generally, smaller grid sizes give results with more accuracy. But due to a small grid size, simulation time increases [14]. It is very important and critical to perform a convergence study on the X and Y grid sizes to provide optimization and the tradeoff between speed and accuracy.

4. Waveguide configuration and analysis

Figure 2 shows the MZIW structure in 3D (XYZ) format with reference to this proposed structure. We can join two *Y* branches (refer **Figure 1**) to form the entire MZIW structure (refer **Figure 2**) [15]. To perform this convergence study, we have used the scanning capabilities of beam propagation method, scanning and optimization tools. The MZI layout under the test is shown in **Figures 3** and **4**.

This scanning tool gives very good results. There are various configurations of photonic MZIW, which are used for sensing various physical parameters [16]. **Figure 3(a–d)** shows the experimental data for light output variation as a function of changes in the branch angle for *Y* branch (1-2).

We can use the proper numerical model for the design of the structure with appropriate characteristics.

Figure 4(a–d) shows experimental data for output variation as a function of changes in the branch angle for inverted *Y* branch (2-1) [17]. The performance of photonics interferometer depends upon various fibre geometry and fibre parameters.

For the successful design and working of sensor, the process of the parameter optimization is very critical and important.

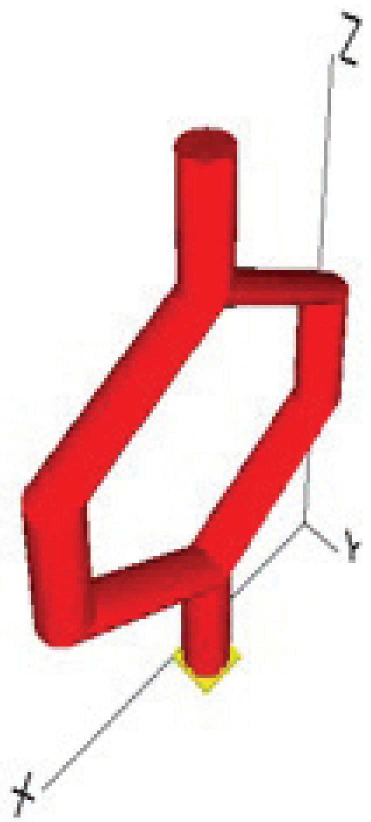

Figure 2. MZIW Structure in 3D format.

We have analysed monitor output behaviour with respect to variations in *Y* branch angle. **Figure 5(a–c)** shows the graph of *Y* branch angle variation versus output value.

From this, it is shown to split light and to combine light at *Y* branches already shown in **Figure 2**. The *Y* branch angle should be optimized. The angle should be less than 18°; above this, light propagation will not be appropriate through the MZIW structure. This reduces the output monitor value [18].

Also when light is guided through the bend structure, substantial radiation losses take place and significant distortion of the optical input launch field occurs when light proceeds through the MZIW structure [19]. As shown in **Figure 5(a)**, as we vary angle between 0° and 25°, monitor output value decreases, and as we increase angle variation beyond 25° that is up to 45°, monitor output value further decreases. This is represented in the graph shown in **Figure 5(b)**. In **Figure 5(c)** as we increase angle variation beyond 45° that is up to 75°, the monitor output value further goes on reducing.

The measuring sensitivity of the MZI structure is given by Eq. (1):

$$S = \frac{\Delta P}{\Delta n} \tag{1}$$

where ΔP is the monitor output power and Δn is the refractive index change at measuring branch.

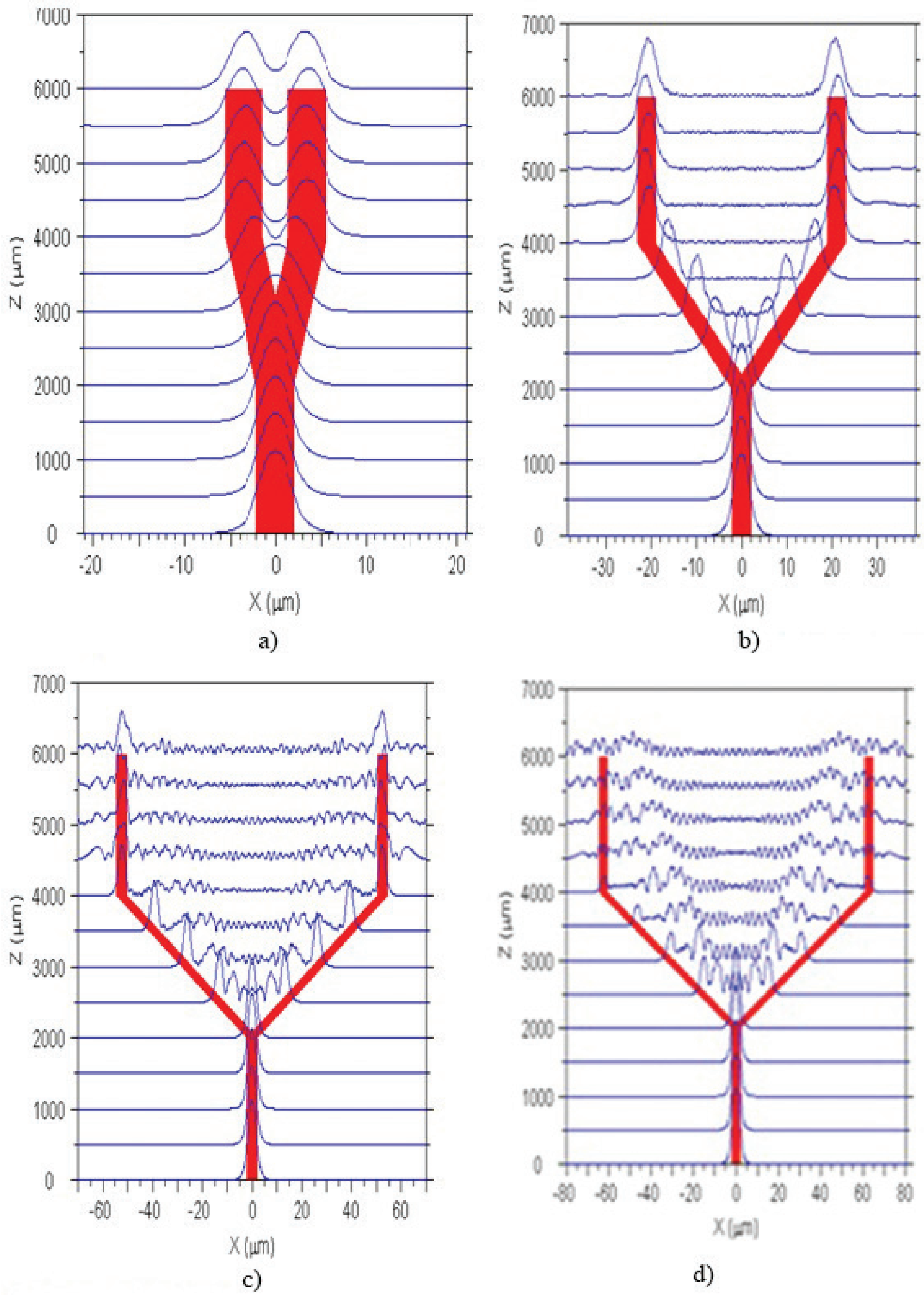

Figure 3. (a) Light guiding variation for *Y* branch at an angle of 18°; (b) light guiding variation for *Y* branch at an angle of 25°; (c) light guiding variation for *Y* branch at an angle of 45° and (c) light guiding variation for *Y* branch at an angle of more than 75°.

From **Figure 5(a–c)**, it is easily interpreted that beyond 18° it is difficult to guide light to the waveguide. These losses depend on the branching angle and increase as the angle increases.

Figure 6(a and **b)** shows the complete MZIW structure after optimum selection of *Y* branch angle (18°) for both the branches. This waveguide has a width of 3 µm and length of 40 µm. This structure is used for sensing applications like refractive index measurement of small

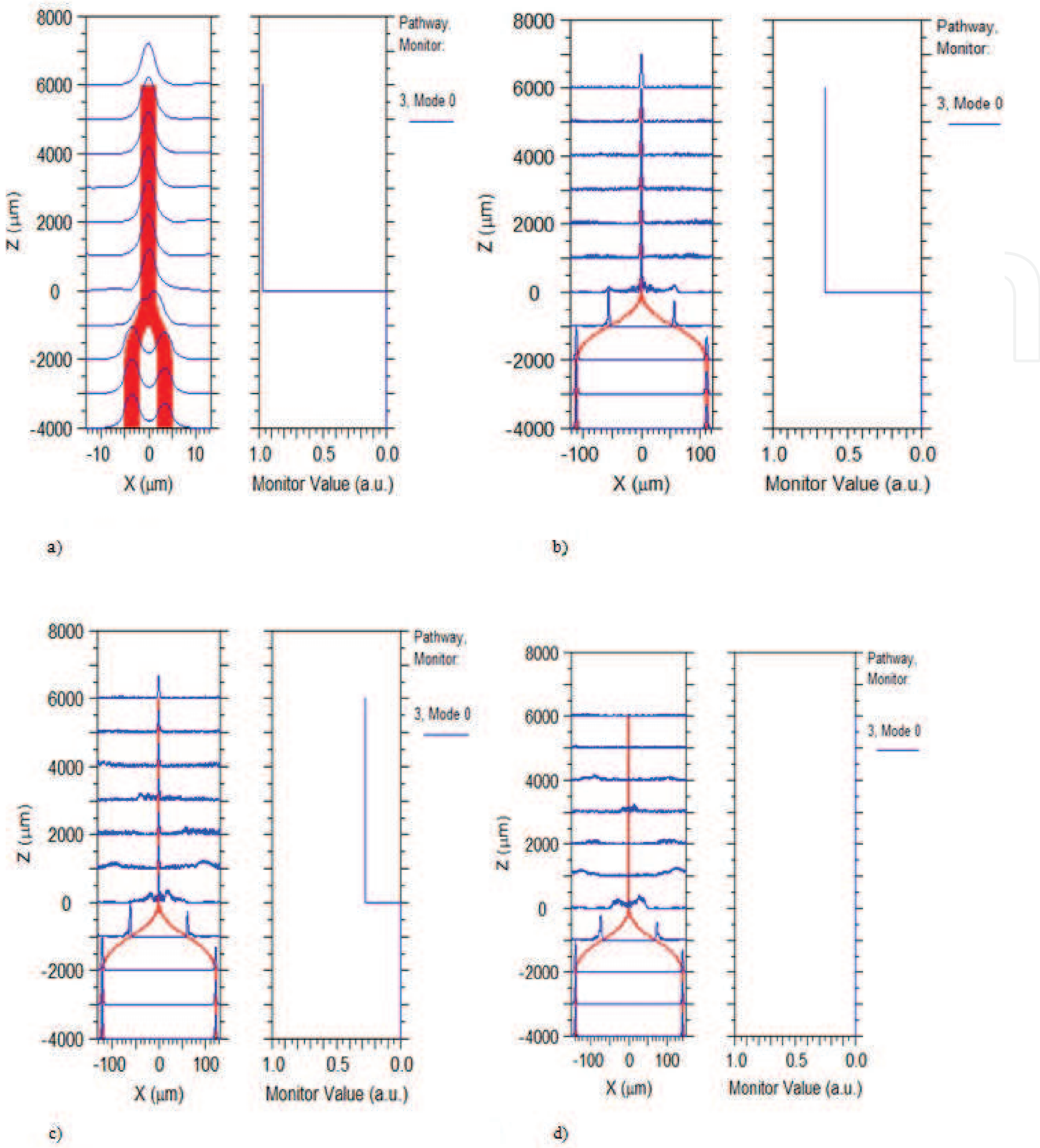

Figure 4. (a–d) Experimental data for output variation as a function of changes in branch angle for inverted *Y* branch (2-1). (a) Light guiding variation for *Y* branch at an angle of 18°; (b) light guiding variation for *Y* branch at an angle of 60°; (c) light guiding variation for *Y* branch at an angle of 75°; and (d) light guiding variation for *Y* branch at an angle more than 75°.

samples under measurement. The validation of the innovative approach is achieved by the characterization of the above MZIW structure. The sensitivity of the sensors is the most dominating and demanding parameter as it directly relates to how early the sensing parameters are detected [20].

According to the theory of interferometer, the intensity modulation scheme should be characterized by an output intensity of MZI behaving as a cosine function of the phase variation as shown in **Figure 5**. Indeed the detected light output power I_{out} at the output of the *Y* branch (2-1) of the interferometer can be detected as given by Eq. (2).

$$I_{out} = I_r + I_{s+2\surd} I_s I_r \cos(\Delta\varphi) \quad (2)$$

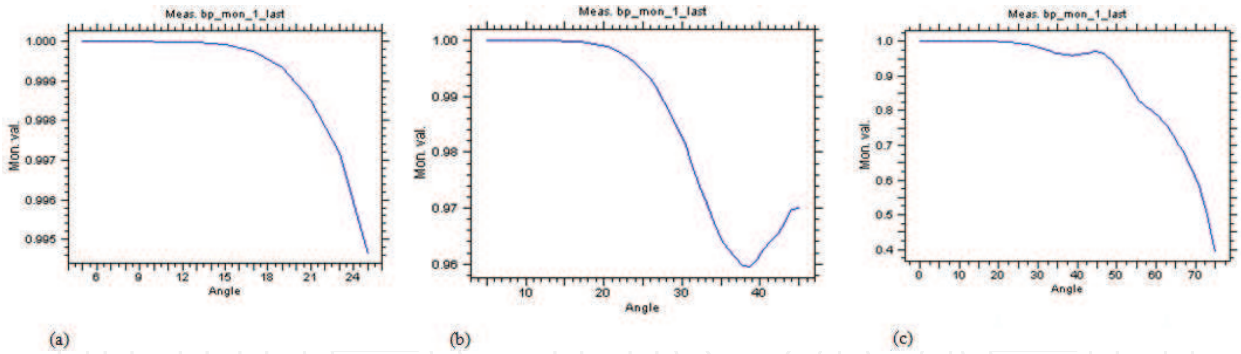

Figure 5. (a–c) Graph of angle variation between 0 and 75°. (a) Output value for angle variation between 0 and 25°; (b) output value for angle variation between 0 and 45°; (c) output value for angle variation between 0 and 75°.

where I_r and I_s are the optional powers of the reference and sensing waveguide observed in each arm of MZIW and $\Delta\phi$ is the phase difference between both waveguides.

The above result and study elucidates the influence of the *Y* branch angle on light guiding the MZIW structure and the MZIW variation in the angle changes light guiding efficiency, so the angle must be properly selected for sensing applications. From the above analysis and experimentation, it is observed that the optimum value for the angle is required to be below 18° (for 1-2 branch). In case of the MZIW interferometer, we know that one arm of the waveguide structure is acting as a reference arm and other arm is acting as a measurement arm. According to the graphs shown in **Figure 5(a–c)**, if light is not properly guided into the reference arm and other measurement arms of waveguides, it will produce considerable variations in the output monitor value. Due to these variations, the physical parameter that is to be

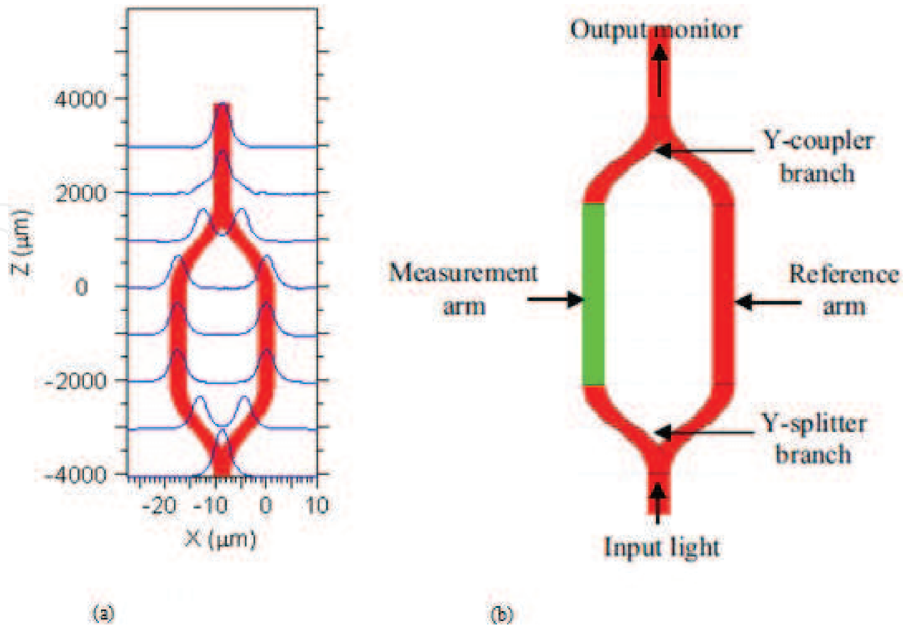

Figure 6. (a) MZIW structure using two *Y* branches and (b) complete MZIW structure used for sensing application.

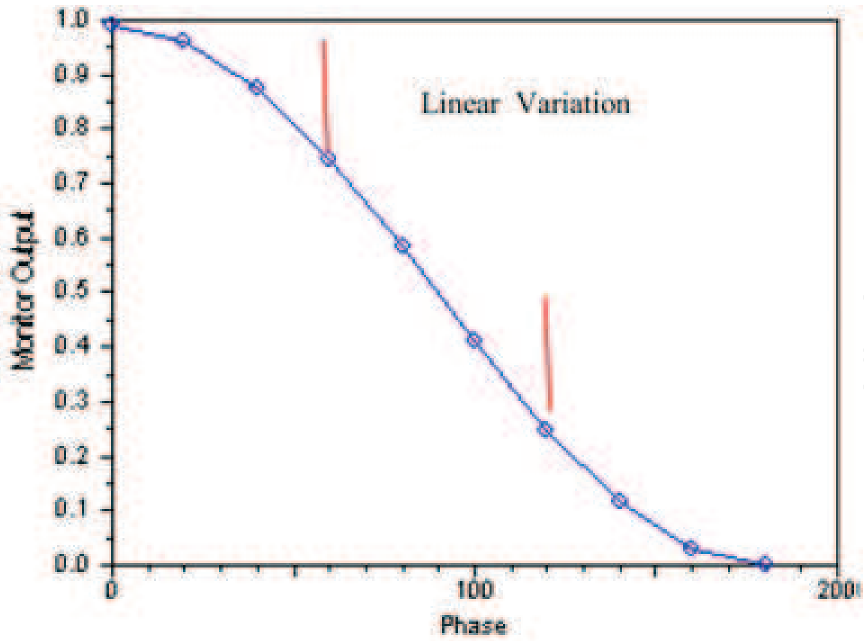

Figure 7. Graph of variation in phase shift and monitor output value for MZIW structure shown in **Figure 6**.

sensed using the interferometer will not be detected correctly. Output measurement becomes difficult. These types of waveguide structures are applicable to any measurement application that changes phase and amplitude of light passing through the waveguide. Generally branch angle should be maintained below 1 radian to reduce insertion losses below 1 dB and 18° for measurement applications.

Analysis and experimental characterization of MZIW is performed using a "beam propagation method" algorithm. Measurement is carried out by using an MZIW structure having branch angle as 18° (for the *Y* branch); however, the insertion loss of power divided also increases rapidly and often becomes intolerable after three or four bifurcation stages.

After the optimization of MZIW for the measurement application is completed, the next part is to analyse the structure for the refractive index (RI) measurement. **Figure 7** shows the phase shift variation due to refractive index variation and corresponding changes in the output monitor value. Due to proper light splitting and combining, changes in phase shift produced due to variations in the refractive index of the sample can be measured.

5. Conclusion

Measurements are carried out by using an MZI structure having branch angle of 18° (for the *Y* branch); however, the insertion loss of power divided also increases rapidly and often becomes intolerable after three or four bifurcation stages. The next step of this chapter consists of the characterization of rib waveguide-based MZI optical sensor.

Acknowledgements

The authors would like to thank University of Pune and also appreciate the help extended by the University for providing funding under the Research and Development Program for this proposed research study work [Reference: BCUD/14, 2008–2010].

We also thank the Management of Dr. D.Y. Patil Institute of Technology, Pune, and S.G.G.S. Institute of Engineering and Technology, Nanded, for providing the necessary facilities for carrying out this work.

Author details

Prashant Bansilal Patel[1]* and Satish T. Hamde[2]

*Address all correspondence to: prashantbgpatel@gmail.com

1 Dr. D.Y. Patil Institute of Technology (DIT), Pune, Maharashtra, India

2 S.G.G.S. Institute of Engineering and Technology (SGGSIET), Nanded, Maharashtra, India

References

[1] Patel PB, Hamde ST. Analysis of the Mach-Zehnder interferometer waveguide structure for refractive index measurement. Journal of Optics. 2017;**46**(4):398-402

[2] Yuan D, Dong Y, Liuand Y, Li T. Mach-Zehnder interferometer biochemical sensor based on silicon-on-insulator rib waveguide with large cross section. Sensors. 2015;**15**: 21500-21517

[3] Weisser M, Tovar G, Mittler-Neher S, Knoll W, Brosinger F, Freimuth H, Lacher M, Ehrfeld W. Specific bio-recognition reactions observed with an integrated Mach-Zehnder interferometer. Biosensors and Bioelectronics. 1999;**14**:409-415

[4] Bosch ME, Sánchez AJR, Rojas FS, Ojeda CB. Recent development in optical fiber biosensors. Sensors. 2007;**7**:797-859

[5] Patel PB, Hamde ST. Characterization of the properties of optical wavefields—An investigations. Journal of Environmental Research and Development (JERAD). 2009;**4**(2):1-2

[6] Patel PB, Hamde ST. Miniaturized Fiber Optic Integrated Biosensor Platforms for Human Health Monitoring, International Conference on Emerging Technologies and Application in Engineering, Technology and Sciences (ICETAETS-08) at Saurashtra University; 13 and 14th January-2008; Rajkot, Gujrat

[7] Heideman RG, Kooyman RPH, Greve J. Performance of a highly sensitive optical waveguide Mach-Zehnder interferometer immunosensor. Sensors & Actuators B. 1993; **10**:209-217

[8] Hu MH, Huang JZ, Scarmozzino R, Levy M, Osgood RM. Tunable Mach-Zehnder polarization splitter using height-tapered Y-branches. IEEE Photonics Technology Letters. 2001;**6**:09

[9] Greivenkamp JE, editor. Handbook of Optics. Vol. 1. 2nd ed. University of Arizona, Tucson, Arizona: Interference, Optical Science Centre. Chapter 2

[10] Estevez MC, Alvarez M, Lechuga LM. Integrated optical devices for lab-on-a-chip biosensing applications. Laser & Photonics Reviews. 2012;**6**:463

[11] Sasaki H, Shiki E, Mikoshiba N. Propagation characteristic of optical guided waves in asymmetric branching waveguides. IEEE Journal of Quantum Electronics. 1981;**QE-17**(6): 1051-1057

[12] Thylen L. The beam propagation method: An analysis of it applicability. Optical and Quantum Electronics. 1983;**15**:433-439

[13] Neyer A, Mevenkamp W, Thylen L, Bo L. A beam propagation method analysis of active and Pasive waveguide crossing. IEEE Journal of Lightwave Technology. 1985;**LT-3**(3): 635-642

[14] Doerr CR. Beam propagation method tailored for step-index waveguides. IEEE Photonics Letters. 2001;**13**(2):2-3

[15] Patel PB, Hamde ST. Photonics sensing techniques based on various Mach Zehnder Interferometer Waveguide (MZIW) structures. In: International Conference on Biomedical Engineering; NIT Jalandhar; 17-19th Dec, 2010

[16] Qi Z-m, Matsuda N, Itoh K, Murabayashi M, Lavers CR. A design for improving the sensitivity of a Mach-Zehnder interferometer to chemical and biological measurements. Sensors and Actuators, B. 2002;**81**:254-258

[17] Sethi RS. Transducer aspects of biosensors. Biosensors & Bioelectronics. 1994;**9**:243-264

[18] Iqbal M, Gleeson MA, Spaugh B, Tybor F, Gunn WG, Hochberg M, Baehr-Jones T, Bailey RC, Gunn LC. Label-free biosensor arrays based on silicon ring resonators and high-speed optical scanning instrumentation. IEEE Journal of Selected Topics in Quantum Electronics. 2010;**16**:654-661

[19] Adams MJ. An Introduction to Optical Wave Guides. Chapter 7. New York: Wiley;

[20] Levy R, Peled A, Ruschin S. Waveguided SPR sensor using a Mach-Zehnder interferometer with variable power splitter ratio. Sensors and Actuators B. 2006;**119**:20-26